Exclusive Operation Strategy for the Supervisory Control of Series Hybrid Electric Vehicles

Wassif Shabbir and Simos A. Evangelou

***Abstract*—Supervisory control systems (SCSs) are used to manage the powertrain of hybrid electric vehicles (HEV). This paper presents a novel SCS called Exclusive operation strategy (XOS) that applies simple rules based on the idea that batteries are efficient at lower loads while engines and generators are efficient at higher loads. The XOS is developed based on insights gained from three conventional SCSs for series HEVs: Thermostat control strategy (TCS), Power follower control strategy (PFCS) and Global equivalent consumption minimization strategy (GECMS). Also, recent technological developments have been considered to make the XOS more suited to modern HEVs than conventional SCSs. The resulting control decisions are shown to emulate the operation of approximate global optimal solutions and thus achieve significant improvement in fuel economy as compared to TCS and PFCS. In addition, the generally linear relationship between required power and engine power for the XOS provides auditory cues to the driver that are comparable to conventional vehicles, thus reducing barriers to adopting HEVs. The simplicity and effectiveness of the XOS makes it a practical SCS.**

I. Introduction

Across the world, there are growing concerns regarding climate change, air pollution and the finite supply of fossil fuels. This has led manufacturers, regulators and consumers to push the whole automotive industry through a historical transition towards an electrified vehicle fleet. A significant step in this process has been the wide range of launches of hybrid electric vehicles (HEVs) that is improving the fuel economy of vehicles on the road. It is estimated that approximately 18% of new vehicles sold in Europe in 2020, and 7% in the US, will be HEVs (the estimates are 8% and 2% respectively for pure electric vehicles) [1]. It is therefore of great interest to study how the benefits of a hybrid powertrain can be maximized.

Researchers have therefore been studying the energy management problem, which involves determining the optimal power share between multiple sources in a hybrid powertrain. This is the responsibility of the supervisory control system (SCS) of the vehicle. A vast range of SCSs have been proposed in the past, ranging from rule-based to optimization based control strategies [2]–[9]. The former are often based on heuristics while the latter use a more sophisticated approach to the control design. However, whenever a new SCS is designed and proposed, it is often compared and evaluated against certain benchmark systems. For series HEVs, the Thermostat control system (TCS) and the Power follower control strategy (PFCS) are the two most conventional SCSs that were proposed almost two decades ago and have since remained the default control systems for benchmarking purposes [10]–[14].

W. Shabbir and S. A. Evangelou are with the Department of Electrical and Electronic Engineering, Imperial College London, United Kingdom (e-mail: wassif.shabbir07@imperial.ac.uk; s.evangelou@imperial.ac.uk)

Supporting data available on request from cap-publications@imperial.ac.uk.

However, hybrid vehicles have changed since these SCSs were introduced. More processing power is available (at little cost and weight), so optimization based solutions are more attractive. Start-stop systems (SSS) have become a standard component and are much more efficient now, so the objective to minimize engine-start events is not as important anymore. The hybridization of the powertrain has tended towards more electrification, meaning that it is no longer sensible to solely focus on optimizing the engine-generator set. All of these factors have been considered, to propose the Exclusive operation strategy (XOS) in this paper. It uses the principle of using the battery at lower loads (where its efficiency is high) and the engine-generator set at higher loads (where its efficiency is high). It will be shown that the fuel economy delivered by the XOS is significantly better than the TCS and PFCS.

More recently, it has also become common to benchmark the performance against a global optimal controller, commonly implemented with dynamic programming [15], [16]. Although such SCSs are impractical for real-time applications due to computational burden, they serve an important role to indicate the bound of performance that is realizable. This approach is however only realistically feasible for simpler vehicle models that can be solved quickly (either analytically or numerically). For more complex models, it is more effective to employ approaches such as a Global equivalent consumption minimization strategy (GECMS), that has been globally tuned to perform practically like a dynamic programming solution [17]. The XOS has taken inspiration from the control decisions of the GECMS in forming its own simpler control rules, and is shown to be only marginally inferior in terms of fuel economy.

The next section introduces the vehicle model used in this paper. Section III describes, designs and implements four distinct SCSs that are simulated to evaluate results in terms of power profiles, state of charge (SOC) and fuel economy in Section IV. Finally conclusions are drawn in Section V.

II. Vehicle Model

The vehicle model described in [18], [19] is used to design and simulate the SCSs presented in this work. The model represents a general-purpose passenger car and consists of a series hybrid powertrain arrangement as shown in Fig. 1. This dynamic model is capable of realistic transient response in the frequency range appropriate for standard driving. The powertrain of the vehicle comprises three branches: the Propulsion Load (PL) which is an inverter driven Permanent Magnet Synchronous Motor (PMSM), mechanically connected to the wheels of the car via a continuously variable transmission; the Primary Source of energy (PS) which consists of a turbocharged 2.0L diesel internal combustion engine (ICE),

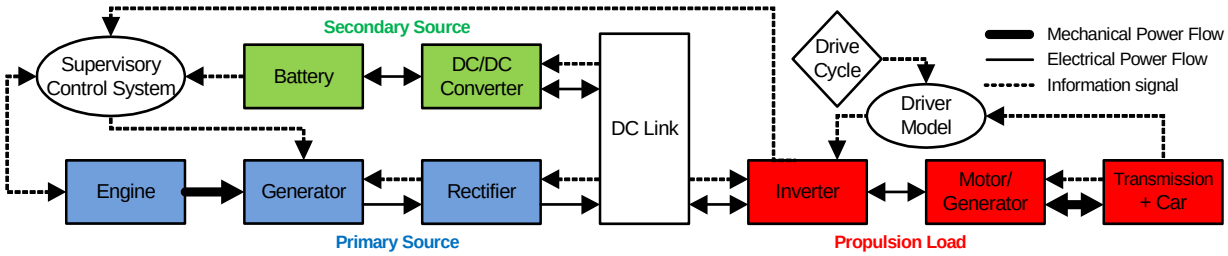

Fig. 1. Overall structure of the series HEV powertrain. The direction of the arrows shows the direction of the power and information flow. [18]

mechanically coupled to a Permanent Magnet Synchronous Generator (PMSG) which is electrically connected to a three-phase rectifier; and the Secondary Source of energy (SS) which contains a lithium-ion battery connected to a bi-directional DC-DC converter. Regenerative braking is possible by the PMSM behaving as a PMSG while capturing the kinetic energy from the wheels and converting it to electrical energy, which then gets stored in the SS. The PL is powered by the PS and SS, all connected to a common DC bus through which energy transfer takes place, giving

$$P_{PS} + P_{SS} = P_{PL}, \tag{1}$$

where P_{PS} and P_{SS} are the output powers of the PS and SS respectively, and P_{PL} is the load power requested by the PL. The paper will use the power share factor u, defined as

$$u = \frac{P_{PS}}{P_{PL}}, \tag{2}$$

giving a single decision variable to determine both P_{PS} and P_{SS} for a given P_{PL}. Both the PS and SS are constrained to operate within upper bounds, which are defined to be $P_{PSmax} = 34$ kW and $P_{SSmax} = 30$ kW respectively. The SS also has a lower bound of $P_{SSmin} = -30$ kW. For all SCSs presented, the SOC is constrained to operate between $SOC_L = 50\%$ and $SOC_U = 80\%$, and is initialized at the mid-point between SOC_L and SOC_U ($SOC_{initial} = 65\%$). The vehicle also includes a start-stop system that enables the ICE to be switched off to reduce idling losses. Also, for all SCSs, the engine speed is controlled optimally for any given PS power as $\omega_{ICE}(P_{PS})$ by a separate engine control, as is often done for series HEVs. Thus, the SCS does not need to control the engine speed.

III. Supervisory Control Systems

The role of the SCS is to determine the power share factor u, given the power requirement P_{PL} and the SOC. This section presents the design and implementation of four different SCSs: TCS, PFCS, GECMS and XOS.

A. Thermostat Control Strategy

The Thermostat control strategy (TCS) is a simple, robust SCS that achieves a good fuel economy and is the most conventional control strategy for series HEVs. The basic principle is to run the PS at its optimal point and have the SS act as an equalizer, as

$$P_{SS} = P_{PL} - P_{PSopt} \tag{3}$$

where P_{PSopt} is the most power efficient point of operation of the PS. This mode of operation is valid until the SOC reaches its upper threshold (SOC_U), at which point it enters a mode of SS-only operation. This mode quickly depletes the SS and once the SOC hits the lower threshold (SOC_L) it returns to operate the PS at its optimal point. This logic is implemented by $S(t)$, which is the state determining whether the PS is generally active ($S(t) = 1$) or not ($S(t) = 0$):

$$S(t) = \begin{cases} 0 & SOC(t) \geq SOC_U \\ 1 & SOC(t) \leq SOC_L \\ S(t^-) & SOC_L < SOC(t) < SOC_U \end{cases}, \tag{4}$$

where $S(t^-)$ is the state S in the previous time sample. Note that the PS will be requested to supplement power (at $P_{PS} = P_{PSopt}$) if the load power exceeds the capability of the SS ($P_{PL} > P_{SSmax}$), without changing $S(t)$ to 1. For the purpose of stable operation an additional rule is also introduced: the PS reduces its supply of power to a lower level (tuned to be $P_{PSmin} = 7$ kW) during the event of regenerative braking, to avoid overcharging the battery.

To determine P_{PSopt}, the efficiency of the PS is studied as a whole (essentially the product of the ICE, PMSG and rectifier efficiencies). This efficiency map is obtained in [18], and it is found that the point of highest efficiency occurs at 22 kW. The implementation of this two-state SCS is best fulfilled using a state machine.

B. Power Follower Control Strategy

The second most conventional SCS for series HEVs is the Power follower control strategy (PFCS). Rather than using the ICE at its most efficient point of operation, the PFCS generally has the PS follow the load of the PL, with some deviation to correct and consider the varying SOC. When the load from the motor (P_{PL}) is low and SOC is high, the SS is selected to deliver the power to the vehicle ($S(t) = 0$). Conversely, when P_{PL} is high or SOC is low, the PS is selected to meet the load ($S(t) = 1$). These states are defined as follows:

$$S(t) = \begin{cases} 0 & SOC(t) \geq SOC_U \text{ and } P_{PL} < P_{PSmin} \\ 1 & SOC(t) \leq SOC_L \text{ or } P_{PL} > P_{SSmax} \\ S(t^-) & SOC(t) \geq SOC_L \text{ and } P_{PL} < P_{SSmax} \end{cases}. \tag{5}$$

For $S(t) = 0$, we always have $P_{PS} = 0$. For $S(t) = 1$, the operation of the PS is defined as

$$P_{PS}(t) = \begin{cases} P_{PSmin} & SOC(t) \geq SOC_U \\ P_m(t) & SOC_L < SOC(t) < SOC_U \\ P_{PSmax} & SOC(t) \leq SOC_L \end{cases} \tag{6}$$

where $P_m(t)$ is given by

$$P_m(t) = P_{PL} + P_{ch}\left(SOC_{initial} - SOC(t)\right). \quad (7)$$

It can be understood that the PS power is essentially following the load P_{PL} when the SOC is at the midpoint between SOC_L and SOC_U, but biases the operation in favor of charging or discharging the SS in the cases of low and high SOC respectively. The bias is scaled by P_{ch} to achieve charge sustaining operation ($P_{ch} = 0.5$ in this work). In general, $P_{SS} \neq 0$ when $S(t) = 1$. The implementation of the rules is done with the Stateflow tool in Simulink. Note that the PS is constrained to operate within $P_{PSmin} \leq P_{PS} \leq P_{PSmax}$ ($P_{PSmin} = 7$ kW is determined through tuning) when it's on.

C. Global Equivalent Consumption Minimization Strategy

The equivalent consumption minimization strategy (ECMS) has been widely described in the literature, both as a proposed SCS as well as for benchmarking [20]–[22]. There are many variants, but the present work implements a globally tuned ECMS (GECMS), based on [21]. It has been shown that such a GECMS is able to realize operation almost identical to the global optimal solution as determined through dynamic programming [17]. This makes the GECMS a very suitable benchmark, as it provides a close to optimal solution to benchmark any proposed SCS without needing to employ dynamic programming. As the principles of ECMS, and its foundation on Pontryagin's Minimum Principle, have been discussed previously in the literature, this section will focus on its implementation, and insights informing the XOS design.

The objective of a GECMS is to minimize the total equivalent fuel consumption (EFC), which is defined as

$$m_{eq} = \int_o^{t_f} \dot{m}_{eq}\, \mathrm{d}t, \quad (8)$$

$$\dot{m}_{eq} = \begin{cases} \dot{m}_f(P_{PS}) - s_d \frac{P_{SS}}{Q_{LHV}} & P_{SS} \geq 0 \\ \dot{m}_f(P_{PS}) - s_c \frac{P_{SS}}{Q_{LHV}} & P_{SS} < 0 \end{cases}, \quad (9)$$

where $\dot{m}_f$ is the fuel consumption rate of the ICE in the PS and Q_{LHV} is the lower heating value of the fuel. The two constants s_d and s_c are equivalence factors that translate the energy discharged/charged by the SS into a corresponding amount of fuel consumed/stored. The values of these constants can be determined by trial-and-error or numerical optimization, to identify the optimal selection of equivalence factors for each driving cycle being tested. Although such tuning can be time-consuming for complex vehicle models, it is likely to be faster and simpler than implementing alternative global SCSs.

The optimization problem is first reduced to a local minimization problem as follows:

$$P_{GECMS} \begin{cases} \min\limits_u \dot{m}_{eq}(t,u)\ \forall t \in [0, t_f] \\ 0 \leq u \leq \frac{P_{PSmax}}{P_{PL}} \end{cases}. \quad (10)$$

However, as the EFC at any given time instant is determined by the power requested by the PL and the power split between PS and SS, the optimization problem can be reformulated as

$$P_{GECMS} \begin{cases} \min\limits_u \dot{m}_{eq}(P_{PL},u)\ \forall P_{PL} \in [0, P_{PLmax}] \\ 0 \leq u \leq \frac{P_{PSmax}}{P_{PL}} \end{cases}, \quad (11)$$

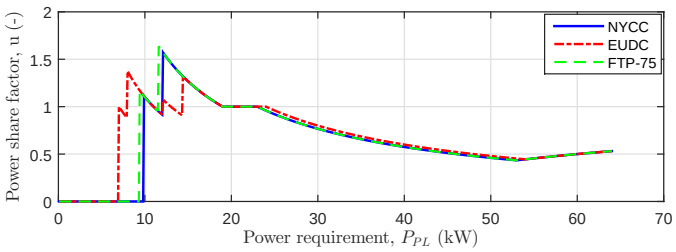

Fig. 2. Power share factor u_{opt} for GECMS for varying power requirement P_{PL}, for three different driving cycles.

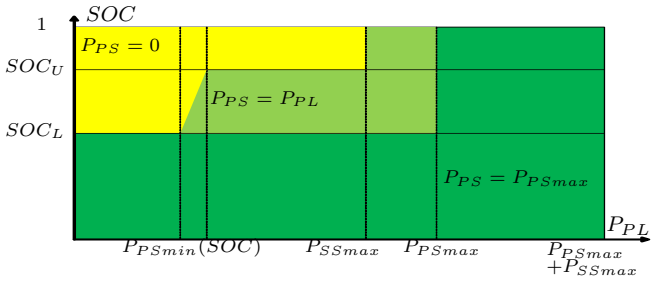

Fig. 3. The XOS operates in three main modes, depending on given SOC and P_{PL}: SS-only, PS-only and hybrid-mode.

where $P_{PLmax} = P_{PSmax} + P_{SSmax}$. Thus, for any given positive power requirement P_{PL}, an optimal power share factor u_{opt} can be defined for each set of equivalence factors s_d and s_c. Using a map of fuel consumption $\dot{m}_f(P_{PS})$, a sweep can be performed for (9) with $u \in [0, \frac{P_{PSmax}}{P_{PL}}]$ and $P_{PL} \in [0, P_{PLmax}]$ to produce an optimal control map [23], [24]. This process is repeated for each candidate set of s_d and s_c. For m number of s_d values and n number of s_c values investigated, there are $m \times n$ number of control maps produced. Finally, each of these control maps are applied to the vehicle model for different driving cycles to identify the best combination of s_d and s_c to minimize m_{eq} for each driving cycle. The resulting optimal control maps are shown in Fig. 2. The GECMS is implemented in Simulink through a simple look-up table that uses the produced map and the requested P_{PL} to select the optimal power share factor, that is then multiplied by P_{PL} to provide the optimal P_{PS}.

D. Exclusive Operation Strategy

Similar to the TCS and PFCS, the Exclusive operation strategy (XOS) is based on heuristic rules. It uses insights gained from TCS and PFCS, and attempts to emulate the operation of optimization-based SCSs, such as the GECMS. But most importantly, investigation of the power-split between the PS and SS in a powertrain shows that the optimal selection is often to operate with the SS at lower powers and the PS at higher load requirements. This agrees roughly with previously developed control systems [23] as well as the GECMS presented here. Thus, the principle of XOS is quite simple: operate with only SS at low load requirements or if ($SOC > SOC_U$), and operate with only PS at medium loads. The two energy sources are only used together if the load power exceeds the maximum rating of the source in operation (or $SOC < SOC_L$). These rules are shown visually in Fig. 3.

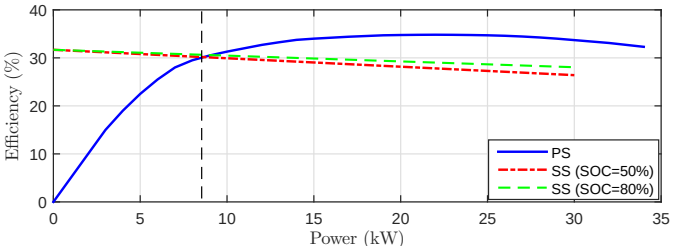

Fig. 4. Efficiency profiles for PS and SS (corrected by η_{re}). The intersection between the profiles is marked by a checked line, corresponding to P_{th}.

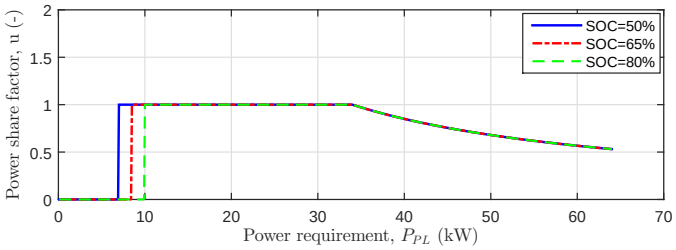

Fig. 5. Power share factor u_{opt} for XOS for varying load P_{PL} and SOC.

The XOS is inspired by the PFCS as can be seen by its "power following" behavior during PS-only mode. However, the XOS does not adjust PS power to correct SOC deviation as done by P_m with the PFCS. Instead the SOC correction is performed by making P_{PSmin} a function of SOC, such that the use of SS is encouraged for higher SOC. Unlike the TCS and PFCS that operate in two distinct states, and thus are implemented with state machines, the XOS has a single state of operation and can be implemented with simple logic gates.

The XOS requires three parameters: $P_{PSmin}(SOC)$, P_{PSmax} and P_{SSmax}. The two latter are readily available for any powertrain, but the former needs some further attention. The threshold $P_{PSmin}(SOC)$ is the load at which the SCS switches from using the SS to PS, and is defined as

$$P_{PSmin}(SOC) = P_{th} + X_{csi}\,(SOC - SOC_{initial}) \quad (12)$$

where P_{th} is the power threshold and X_{csi} regulates the charge sustaining intensity of the SCS (for $SOC \in [SOC_L, SOC_U]$). To determine the optimal value for P_{th}, the efficiencies of the SS and PS should be compared. However, as the SS efficiency by itself does not consider the PS losses required to replenish the SS, a correction factor η_{re} is included, which is similar to the average operating PS efficiency. This has been found to be $\eta_{re} = 33\%$ in [23], but could be tuned for any powertrain. Figure 4 shows a comparison of PS and SS efficiencies based on the components used in this work, but similar shapes would be found for most series HEVs. As expected, the SS efficiency is high at low loads and drops for higher loads, while the PS starts with a lower efficiency and moves towards a higher efficiency (peaking at 22 kW). Thus the threshold at which the PS becomes more efficient than the SS if found to be between 8.5 and 9 kW depending on SOC. In this work, $P_{th} = 8.5$ kW was found to deliver optimal fuel economy results.

Lastly, X_{csi} needs to be determined to make the control system charge sustaining. A larger value results in more intense charge sustaining operation, meaning that the SOC profile is less likely to diverge from $SOC_{initial}$, but at the expense of fuel economy. In this work $X_{csi} = 10$ was found to be suitable, meaning that $P_{PSmin}(SOC)$ ranges from 7 to 10 kW (for SOC_L and SOC_U respectively).

A particular benefit of driving with each energy source exclusively is the linear correlation between PL power request and PS power supply. Drivers have developed a sense of intuition with regards to the speed and acceleration of the vehicle based on auditory cues from the ICE in a conventional car. The unfamiliar, and sometimes counterintuitive, cues provided by a hybrid powertrain remain a significant challenge in terms of drivability for adopters of HEVs. The XOS addresses this particular issue, but the switching between PS and SS mode remains a challenge in terms of drivability. However, drivers are increasingly becoming familiar with this sensation as start-stop systems are introduced in conventional vehicles or mild hybrids. The XOS therefore helps in making the driver experience for a HEV more similar to a conventional vehicle.

It is interesting to compare and contrast the operation of the GECMS and the XOS. Each SCS has the same task: to determine the optimal power split of the load request between the PS and SS. This task is reduced to the selection of the power share factor u, as shown for the GECMS in Fig. 2. The equivalent chart for XOS is presented in Fig. 5, for operation with $SOC_L \leq SOC \leq SOC_U$.

It can be seen that the XOS has three simple stages of operation: the first stage (low P_{PL}) is SS-only; the second stage (medium P_{PL}) is PS-only; and the third stage (high P_{PL}) is hybrid mode with the PS delivering maximum power. The transition between the first and second stage is dependent upon the SOC, such that battery use is encouraged at high SOC and discouraged at low SOC. This type of transition is also visible in the same region for the GECMS in Fig. 2. Although the latter is not sensitive to SOC directly, it can be seen that the transition occurs at higher P_{PL} for NYCC to encourage the use of the SS during urban driving, while the transition is at lower P_{PL} for EUDC where PS operation is preferred for highway driving. In the second stage, where XOS applies $u = 1$, the GECMS is slightly higher towards the start of this stage, and slightly lower towards the end of the stage. Operation above the $u = 1$ line can be considered to be SS-charging operation while operation below this line is SS-depleting. Thus, the operation of XOS can be considered a smoothened version of the GECMS operation, to balance out charging and depleting operations. Although not optimal, the simplified control policy of XOS emulates the general behavior of the GECMS, and can thus be expected to perform well.

IV. Results

The four SCSs can now be tested on the described vehicle model to investigate operation and performance and assess the effectiveness of the XOS. Simulations are run for three different driving cycles: the NYCC is low-speed urban driving; the EUDC is European highway driving; and FTP-75 combines urban and high-speed driving. As a single iteration of these driving cycles is quite short, some will be repeated to allow investigation of features exhibited over longer time-frames.

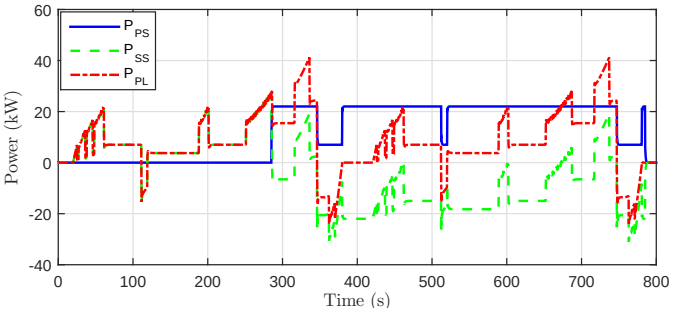

Fig. 6. Power profiles for PS, SS and PL when driving EUDC with TCS.

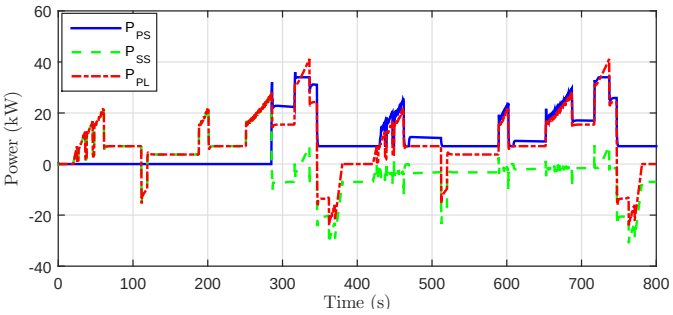

Fig. 7. Power profiles for PS, SS and PL when driving EUDC with PFCS.

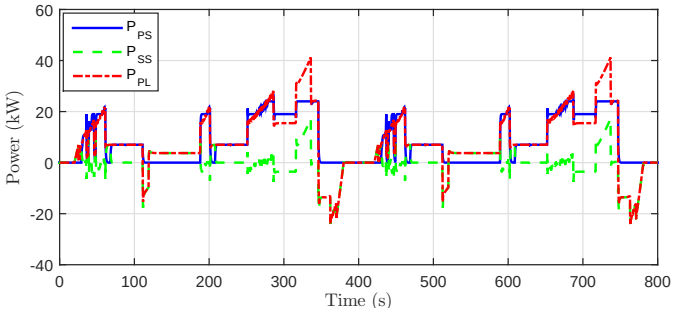

Fig. 8. Power profiles for PS, SS and PL when driving EUDC with GECMS.

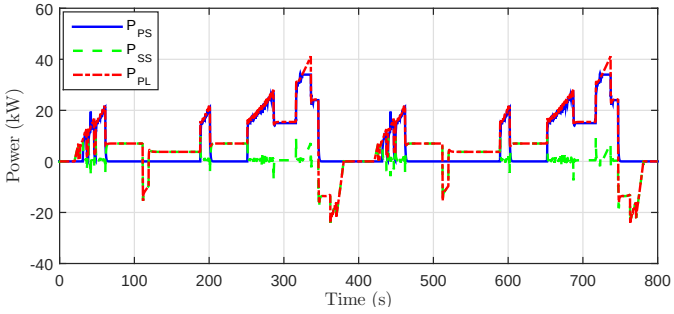

Fig. 9. Power profiles for PS, SS and PL when driving EUDC with XOS.

A. Power Profiles

To investigate the realized power split for each SCS, the power flow through the PS, SS and PL are measured for both urban (NYCC) and highway (EUDC) driving. Figures 6, 7, 8 and 9 illustrate the power time histories (for the P_{PS}, P_{SS} and P_{PL}) for TCS, PFCS, GECMS and XOS respectively for two iterations of the EUDC driving cycle. The double iteration allows the two distinct states of the TCS and PFCS to manifest themselves. Similarly, Figs. 10, 11, 12 and 13 illustrate the power time histories for TCS, PFCS, GECMS and XOS respectively for the first half of the NYCC driving cycle. As urban driving involves more frequent changes in driving operation, it is sufficient to study five minutes of driving to observe the essential features of the SCSs. Also, it allows the charts to be clearer and less crowded with data.

The first 280 seconds of the EUDC driving with TCS are powered fully by the SS, requiring close to the maximum power of the battery. Thereafter the PS is switched on and provides 22 kW constantly, which is its optimal point of operation. There are occasional dips in power from the PS during regenerative braking, to ensure the SS is not overloaded. During this second stage of operation, the battery is almost always being intensively charged, apart from the occasions where the required power P_{PL} exceeds the optimal point of operation of the PS. The urban driving in Fig. 10 on the other hand remains in SS only mode in general and only requires the PS when the load power exceeds the capability of the SS.

Similarly, the PFCS opens the highway driving by operating with SS only, but soon enters its hybrid mode. During cruising at lower speeds ($<$7 kW) the PS operates steadily at minimum power, while during accelerations and high-speed cruising the PS ends up providing all the power apart from during power requirements in excess of the maximum ratings of the PS (34 kW). The PS power profile is essentially following the PL power, but there is an offset (that is proportional to the SOC deviation) that decreases with progression into the driving cycle. It can be noted that the SS power has oscillations whenever there are sudden changes to the load power. Independent of the SCS, the SS will act as an equalizer to balance the power load between the PS and the PL during fast transitions, as the PS has much slower dynamics. During urban driving, in Fig. 11, the same pattern emerges which begins with SS-only operation followed by the PS being consistently on. However, as the power requests are generally very low, the PS ends up operating at its defined minimum operating point (7 kW) until the next change in state.

The GECMS on the other hand uses the SS much more consistently. For the EUDC, during cruising at low speeds (around $<$6 kW) the SS is completely powering the vehicle, while during accelerations and high-speed cruising, the PS ends up providing almost all the power apart from during times of fast transitions or high power requirements ($>$25 kW). For example, between $t = 250$ s and $t = 340$ s the GECMS operates the PS at a different power level than the required power P_{PL} to allow the powertrain as a whole to perform optimally. Similarly, for urban driving it can be seen around $t = 200$ s that the two peaks in P_{PL} are met in hybrid mode as opposed to purely with the PS. This not only allows fuel efficient operation, but also avoids sudden loading of the PS from zero to close to maximum power requests. Also, it is worth noting that the GECMS operates identically for each of the two iterations of the EUDC. The TCS and PFCS operate in vastly different ways due to the non-linear effects of changes in states S as well as variations in SOC.

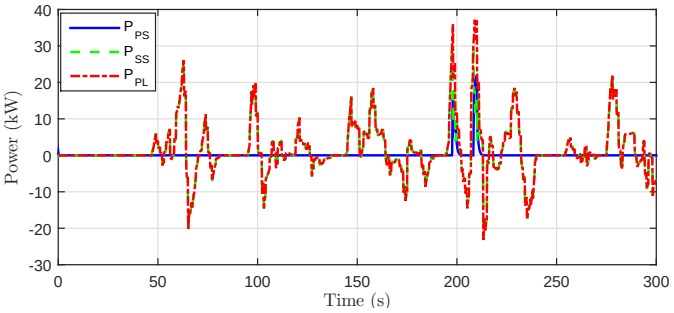

Fig. 10. Power profiles for PS, SS and PL when driving NYCC with TCS.

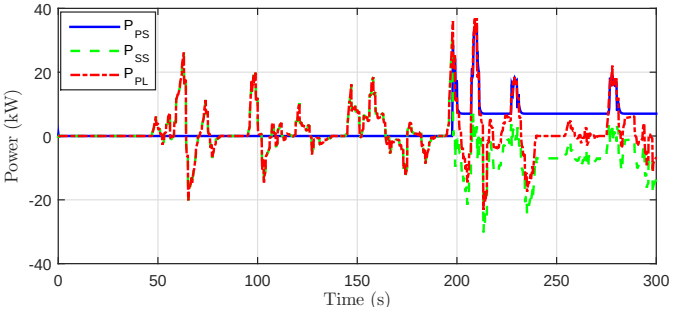

Fig. 11. Power profiles for PS, SS and PL when driving NYCC with PFCS.

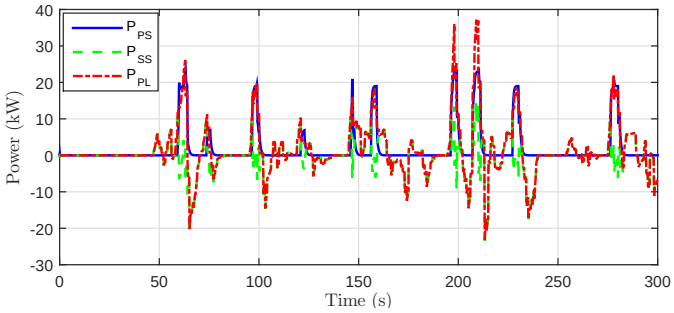

Fig. 12. Power profiles for PS, SS and PL when driving NYCC with GECMS.

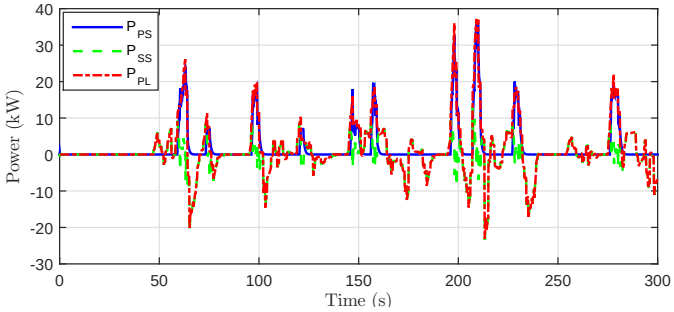

Fig. 13. Power profiles for PS, SS and PL when driving NYCC with XOS.

Lastly, the XOS power profiles show that highway driving is performed quite similarly to GECMS. The PS is used less often (e.g. around $t = 90$ s and $t = 220$ s) than with GECMS and at different magnitudes. Thus, even more than the GECMS, either the PS or the SS power profile often exclusively follows the power requirements of the PL. This demonstrates the previously made point that the XOS makes driving the HEV more similar to a conventional car in terms of auditory cues from the ICE. Also, it is worth noting that unlike all the other SCSs, the XOS never uses the PS to charge the SS directly, but instead it relies on regenerative braking to avoid depletion. This is not an issue for urban driving though, as shown in Fig. 13, where significant regenerative braking is combined with small bursts of using the PS. This requires a significant number of ICE switching, but modern SSS allows this to be done in a fuel efficient manner. The XOS is also sensitive to variations in SOC but to such a limited extent as to not be visible in the presented results.

B. State of Charge Profiles

In addition to studying the power profiles for the different SCSs it is insightful to compare their SOC profiles, which are presented in Figs. 14-16 for the three driving cycles. As SOC is a quite slow dynamic, results for repeated driving cycles have been presented (16×NYCC, 8×EUDC and 4×FTP-75).

The signature zigzagging SOC profile of the TCS is apparent for all three driving cycles as the SS is charged and discharged alternately between the lower and upper SOC boundaries. The high-speed driving of the EUDC produces almost a triangle wave as the charging and discharging powers are quite persistent and balanced. However, as NYCC and FTP-75 are often operated at zero or low powers, the charging of the battery is very rapid when the PS produces 22 kW, producing SOC profiles looking more like sawtooth waves.

Similarly, the PFCS also tends to behave in an oscillating fashion due to its operation in two distinct states, where $S = 0$ often leads to discharging patterns similar to the TCS (for EUDC and FTP-75 in particular). However, the charging at $S = 1$ is significantly less aggressive as is particularly visible for EUDC and FTP-75 where the slope of the SOC profile is quite low during charging operation. However, for NYCC the $S = 1$ operation will result in significant charging of the

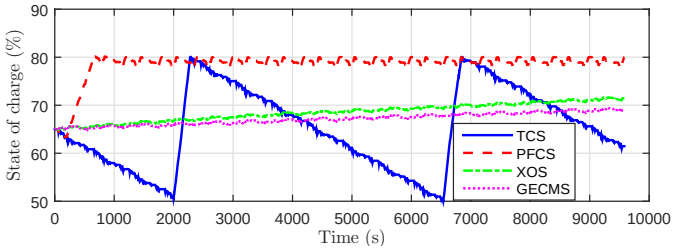

Fig. 14. SOC profiles for the NYCC for the four presented control systems.

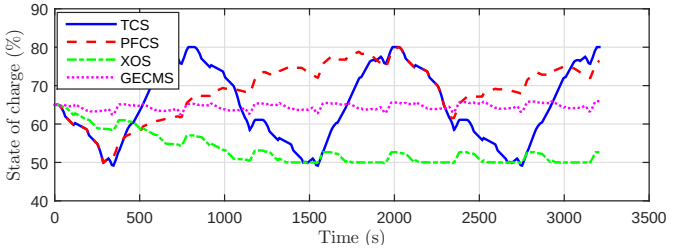

Fig. 15. SOC profiles for the EUDC for the four presented control systems.

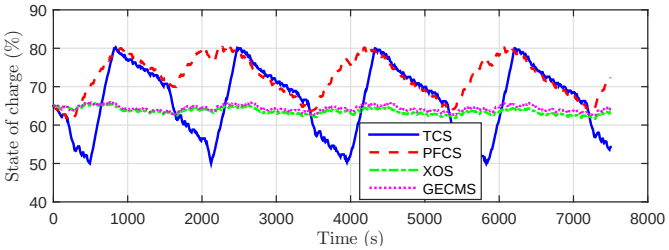

Fig. 16. SOC profiles for the FTP-75 for the four presented control systems.

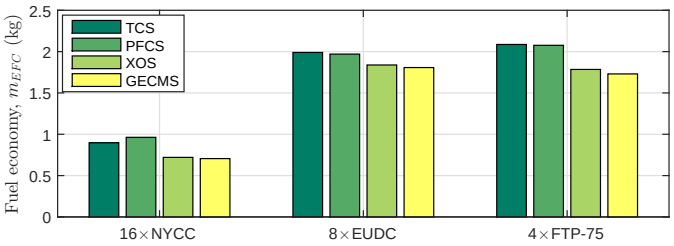

Fig. 17. Comparison of equivalent fuel consumption for TCS, PFCS, XOS and GECMS for repeated iterations of the three driving cycles.

battery until $SOC = SOC_U$ and the state of the controller enters $S = 0$. Thereafter the SOC drops for a short duration before the occasional surge in power requirements will make the PFCS enter $S = 1$ mode again, causing a cycle of charging and discharging with a much shorter period.

The GECMS typically finishes close to $SOC = SOC_{initial}$. The 4% deviation for the NYCC is in fact an exceptional occurrence due to limited precision in tuning. The equivalence factors were tuned for a single iteration of the NYCC, and any minor imprecision is scaled significantly after 16 repetitions. Nevertheless, the GECMS is the most charge sustaining of the SCSs tested in this paper, which suggests that fuel economy in fact generally benefits from charge sustaining operation.

Similarly (and in contrast to the TCS and PFCS), the XOS operates quite steadily and has neither extreme charging nor discharging. For NYCC, the SOC is gradually drifting higher due to the significant amount of regenerative braking. However, this corresponds to a deviation of 7% from SOC_{inital}, which is not much considering the vehicle has performed 2 hours and 40 minutes of urban driving. The SOC deviation is more significant for the highway driving of EUDC, where the limited amount of regenerative braking combined with occasional low-speed cruising result in a gradually depleting battery. Although the XOS has some inherent charge sustaining features (P_{PSmin} is a function of SOC), they are not sufficient to prevent SOC to reach its lower bound, SOC_L. However, once it reaches the lower threshold it starts using the PS more to keep the SOC in an acceptable region. As the vehicle is tested for more mixed driving in FTP-75, the charge is sustained very close to $SOC_{initial}$, as the elements of regenerative braking and low-speed cruising balance each other quite well. This is similar to the GECMS (with some more SOC deviation), again reflecting the fact that XOS operation emulates the behavior of the GECMS.

C. Fuel Economy

To evaluate the fuel economy it is useful to apply the concept of equivalent fuel consumption m_{EFC}, which is similar to m_{eq} used for the GECMS. It allows comparison of the overall fuel economy by considering the actual fuel consumption as well as the shortage/surplus of final SOC. Many analytical methods have been described in the literature to define such an equivalence between SOC and fuel consumption [25]–[27]. For the purposes of analyzing the results in this work, the line-chart approach described in [27] is adopted as it is a natural extension of the ECMS. Using simulated results allows the identification of $s_{d,EFC}$ and $s_{c,EFC}$, such that

$$m_{EFC} = \begin{cases} m_f + s_{d,EFC} \cdot \Delta soc \frac{Q_{max} V_{b,OC}}{Q_{LHV}} & \Delta soc \geq 0 \\ m_f + s_{c,EFC} \cdot \Delta soc \frac{Q_{max} V_{b,OC}}{Q_{LHV}} & \Delta soc < 0 \end{cases}, \tag{13}$$

where $\Delta soc = SOC_{initial} - SOC_{final}$, Q_{max} is the battery capacity and $V_{b,OC}$ is the battery open-circuit voltage.

Simulation results for the fuel economy of the four investigated SCSs are presented in Table I for repeated iterations of each driving cycle. The actual fuel consumption is given together with the final SOC value, and these data points are used to calculate the equivalent fuel consumption m_{EFC}. The final row of the table gives the relative performance of each SCS in terms of fuel economy in relation to the GECMS, which operates close to the global optimal solution. The fuel economy results are also compared visually in Fig. 17.

TCS and PFCS prefer urban and highway driving respectively, but are quite similar in their fuel economy performance. However, they are fully 27.1% and 35.5% worse than the GECMS during urban driving with NYCC. The results are somewhat better for FTP-75, and the relative gap is smallest for highway driving with EUDC. This inferior performance could have been attributed to the simplicity of these SCSs, if it was not for the stark counter-example provided by the XOS results which are just 2-3% behind the GECMS. The results of the XOS are in fact impressively close to the global optimal results, considering the extreme simplicity of the rules.

There are many factors contributing to the XOS being more effective today than it would have been in the past. The core principle of the TCS is to optimize the ICE operation, which used to be valid when the relative marginal cost of using the battery as an equalizer was small. However, not only have ICEs become more efficient with time, it has become increasingly common to connect the battery to the powertrain through a DC-DC converter, which adds another source of loss in the SS. Both of these factors increase the importance of looking beyond just the ICE when determining the desired power split. Additionally, both the TCS and PFCS operate conservatively with regards to switching the state of the ICE between off and on. This switching was historically associated with significant fuel and emission costs, which have been drastically reduced in the past decade. However, high amount of switching still remains undesirable due to its impact on drivability. The presented rules for the XOS take these developments into consideration to deliver improved performance.

TABLE I
COMPARISON OF FUEL ECONOMY

	16×NYCC				8×EUDC				4×FTP-75			
	TCS	PFCS	XOS	GECMS	TCS	PFCS	XOS	GECMS	TCS	PFCS	XOS	GECMS
Fuel [kg]	0.857	1.110	0.783	0.745	2.144	2.109	1.711	1.817	1.963	2.150	1.771	1.725
SOC [%]	61.46	80.02	71.44	69.07	80.04	76.50	52.67	65.95	54.31	72.37	63.62	64.59
m_{EFC} [kg]	0.897	0.963	0.720	0.706	1.990	1.970	1.838	1.807	2.086	2.076	1.784	1.730
Δm_{EFC} [%]	+27.1	+36.5	+2.1	0	+10.1	+9.0	+1.7	0	+20.6	+20.0	+3.1	0

V. CONCLUSIONS

Based on recent developments in hybrid powertrains, start-stop systems and ICE performance, a novel rule-based control strategy has been proposed in this paper, namely the XOS. The XOS development has also used insights from the design and operation of three popular series HEV SCSs: TCS, PFCS and GECMS. The three SCSs have also been presented, to benchmark against the XOS in terms of design, operation, SOC variation and fuel economy in simulations with a diverse range of driving cycles.

It has been shown that the XOS achieves better fuel economy and healthier battery operation than the conventional rule-based control systems, despite using simpler rules. Its performance is not claimed to be better than other real-time feasible optimization SCSs, but the XOS delivers remarkable fuel economy considering its simple nature and ease of implementation. Furthermore, the exclusive operation of each power source allows more intuitive auditory feedback for the driver, improving drivability. However, this simplicity compromises the charge sustaining nature of the SCS, as it is not rigorously charge sustaining if exposed to particularly monotone and aggressive types of driving (although a higher X_{csi} would guarantee charge sustaining operation, but at the expense of fuel economy). Nevertheless, the XOS control has been demonstrated to be charge sustaining for extended periods of typical driving. As such, it appears an appropriate choice to benchmark further control strategies or energy management systems, together with global optimization controllers.

REFERENCES

[1] X. Mosquet, M. Devineni, T. Mezger *et al.*, "Powering autos to 2020: the era of the electric car," *Boston Consulting Group*, 2011.

[2] M. Kim, D. Jung, and K. Min, "Hybrid thermostat strategy for enhancing fuel economy of series hybrid intracity bus," *IEEE Transactions on Vehicular Technology*, vol. 63, no. 8, pp. 3569–3579, 2014.

[3] C. Hou, M. Ouyang, L. Xu, and H. Wang, "Approximate pontryagins minimum principle applied to the energy management of plug-in hybrid electric vehicles," *Applied Energy*, vol. 115, pp. 174–189, 2014.

[4] S. Di Cairano, W. Liang, I. V. Kolmanovsky, M. L. Kuang, and A. M. Phillips, "Power smoothing energy management and its application to a series hybrid powertrain," *IEEE Transactions on Control Systems Technology*, vol. 21, no. 6, pp. 2091–2103, 2013.

[5] K. Çagatay Bayindir, M. A. Gözüküçük, and A. Teke, "A comprehensive overview of hybrid electric vehicle: Powertrain configurations, powertrain control techniques and electronic control units," *Energy Conversion and Management*, vol. 52, no. 2, pp. 1305 – 1313, 2011.

[6] L. V. Pérez and E. A. Pilotta, "Optimal power split in a hybrid electric vehicle using direct transcription of an optimal control problem," *Mathematics and Computers in Simulation*, vol. 79, no. 6, pp. 1959–1970, 2009.

[7] D. Crolla, Q. Ren, S. ElDemerdash, and F. Yu, "Controller design for hybrid vehicles - state of the art review," in *Vehicle Power and Propulsion Conference (VPPC)*, Sept 2008, pp. 1–6.

[8] F. Salmasi, "Control strategies for hybrid electric vehicles: Evolution, classification, comparison, and future trends," *IEEE Transactions on Vehicular Technology*, vol. 56, no. 5, pp. 2393–2404, Sept 2007.

[9] X. He, M. Parten, and T. Maxwell, "Energy management strategies for a hybrid electric vehicle," in *Vehicle Power and Propulsion Conference (VPPC)*, Sept 2005, pp. 390–394.

[10] N. Jalil, N. A. Kheir, and M. Salman, "A rule-based energy management strategy for a series hybrid vehicle," in *American Control Conference, 1997. Proceedings of the 1997*, vol. 1. IEEE, 1997, pp. 689–693.

[11] M. R. Cuddy and K. B. Wipke, "Analysis of the fuel economy benefit of drivetrain hybridization," SAE Technical Paper, Tech. Rep., 1997.

[12] C. Anderson and E. Pettit, "The effects of apu characteristics on the design of hybrid control strategies for hybrid electric vehicles," SAE Technical Paper, Tech. Rep., 1995.

[13] J. Gao, F. Sun, H. He, G. Zhu, and E. Strangas, "A comparative study of supervisory control strategies for a series hybrid electric vehicle," in *Asia-Pacific Power and Energy Engineering Conference (APPEEC)*, March 2009, pp. 1–7.

[14] M. Ehsani, Y. Gao, and A. Emadi, *Modern electric, hybrid electric, and fuel cell vehicles: fundamentals, theory, and design*. CRC press, 2010.

[15] R. M. Patil, Z. Filipi, and H. K. Fathy, "Comparison of supervisory control strategies for series plug-in hybrid electric vehicle powertrains through dynamic programming," *IEEE Transactions on Control Systems Technology*, 2014.

[16] C.-C. Lin, H. Peng, J. W. Grizzle, and J.-M. Kang, "Power management strategy for a parallel hybrid electric truck," *IEEE Transactions on Control Systems Technology*, vol. 11, no. 6, pp. 839–849, 2003.

[17] L. Serrao, S. Onori, and G. Rizzoni, "A comparative analysis of energy management strategies for hybrid electric vehicles," *Journal of Dynamic Systems, Measurement, and Control*, vol. 133, no. 3, p. 031012, 2011.

[18] S. A. Evangelou and W. Shabbir, "Dynamic model for the evaluation of powertrain, transmission and control of hybrid electric vehicles," in *Advances in Automotive Control (AAC)*. IFAC, in review.

[19] S. A. Evangelou and A. Shukla, "Advances in the modelling and control of series hybrid electric vehicles," in *American Control Conference (ACC)*. IEEE, 2012, pp. 527–534.

[20] G. Paganelli, S. Delprat, T.-M. Guerra, J. Rimaux, and J.-J. Santin, "Equivalent consumption minimization strategy for parallel hybrid powertrains," in *Vehicular Technology Conference (VTC)*, vol. 4. IEEE, 2002, pp. 2076–2081.

[21] L. Serrao, S. Onori, and G. Rizzoni, "ECMS as a realization of pontryagin's minimum principle for HEV control," in *American Control Conference (ACC)*. IEEE, 2009, pp. 3964–3969.

[22] B. Geng, J. K. Mills, and D. Sun, "Energy management control of microturbine-powered plug-in hybrid electric vehicles using the telemetry equivalent consumption minimization strategy," *IEEE Transactions on Vehicular Technology*, vol. 60, no. 9, pp. 4238–4248, 2011.

[23] W. Shabbir and S. A. Evangelou, "Real-time control strategy to maximize hybrid electric vehicle powertrain efficiency," *Applied Energy*, vol. 135, pp. 512–522, 2014.

[24] V. Sezer, M. Gokasan, and S. Bogosyan, "A novel ECMS and combined cost map approach for high-efficiency series hybrid electric vehicles," *IEEE Transactions on Vehicular Technology*, vol. 60, no. 8, pp. 3557–3570, 2011.

[25] T. Katrašnik, "Analytical method to evaluate fuel consumption of hybrid electric vehicles at balanced energy content of the electric storage devices," *Applied Energy*, vol. 87, no. 11, pp. 3330–3339, 2010.

[26] L. Guzzella and A. Sciarretta, *Vehicle propulsion systems*, 2nd ed. Springer, 2007.

[27] A. Sciarretta, M. Back, and L. Guzzella, "Optimal control of parallel hybrid electric vehicles," *IEEE Transactions on Control Systems Technology*, vol. 12, no. 3, pp. 352–363, 2004.